Documentation of the Conceptual Design of a

Compact Photon Source (CPS)

E. Chudakov, D. Day, P. Degtiarenko, R. Ent, D.J. Hamilton, T. Horn, D. Keller, C. Keppel, G. Niculescu, P. Reid, I. Strakovsky, B. Wojtsekhowski, J. Zhang

I Executive Summary

This document describes the feasibility of a compact, high intensity photon source (CPS) with large gain in figure-of-merit to be used with dynamically polarized targets to measure processes such as Wide-Angle and Timelike Compton Scattering (WACS and TCS). The design is flexible allowing the CPS to be converted into a K_L beam for spectroscopy experiments. PAC43, PAC44 and PAC45 at Jefferson Lab have seen a few proposals and several LOIs related to these photoproduction topics. One of these is C12-17-008 (Polarization Observables in Wide-Angle Compton Scattering at large s, t, and u), which was conditionally approved w/ Technical Review. The issues stated in the PAC45 report to be addressed are:

- Finalize the design and price estimate for CPS
- Clearly establish the expected maximum photon intensity

This goal of this document is to address these PAC45 technical comments for full approval of C12-17-008.

II Motivation: Science Gain with CPS

A Polarization Observables in Wide-Angle Compton Scattering

The three-dimensional nucleon structure has been an active field, especially during the last two decades since the invention of GPD formalism, and continues to be central to the hadron physics at JLab. GPD formalism provides a unified description of such important reactions as elastic electron scattering, DIS, DVCS/TCS, WACS and several meson production channels. They are all described by a single set of four functions E, H and $\tilde{E}, \tilde{H}$. These functions need to be modeled with parameters which should be determined from the experimental data.

The WACS experimental observables provide several constraints for GPDs which are complementary to other exclusive reactions due to an e_a^2 factor and an additional $1/x$ weighing in the GPD integrals for WACS, e.g. the elastic form factor $F_1(t) = \sum_a e_a \int dx H^a(x,0,t)$ in contrast to the WACS vector form factor $R_V(t) = \sum_a e_a^2 \int \frac{dx}{x} H^a(x,0,t)$, both of which are based on the same GPD $H(x,0,t)$. In addition, for the $\tilde{H}(x,\xi,t)$ the WACS axial form factor $R_A(t)$ provides much more accurate data than an alternative constraint from the nucleon axial form factor.

The experiment needs to be performed at large photon energy and scattering angle where the GPD-based calculations have good and predictable accuracy ($s, -t, -u > 2.5$ GeV^2). The experimental challenges associated with double-polarization measurements of photon-induced reactions at high momentum transfer are formidable. Detector rate capabilities and radiation hardness are both severely tested in beam-recoil measurements as a result of a rapid decrease in recoil proton polarimeter analyzing power at high $-t$. Utilization of a mixed electron-photon bremsstrahlung beam, on the other hand, limits luminosity

in beam-target measurements due to loss of target polarization, primarily as a result of electron-induced heat load. In the preparation of a 12 GeV Jefferson Lab experimental proposal on polarized wide-angle Compton Scattering (WACS), a completely new experimental approach was developed, based on deploying a high-intensity compact photon beam source and a polarized target. This new technique opens up physics possibilities that had hitherto been inaccessible at tagged photon facilities and results in a significantly improved figure-of-merit (of a factor of ∼30) over all previous double-polarization measurements involving photon-induced reactions.

1 Target System and Limitations

We start from the premise that the Compact Photon Source (CPS) target system will be able to handle the the same heat load from the photon beam and the microwaves source as used in electron beam experiments. From the perspective of the low energy production of free radicals in the target material, this approximation is expected to be good within 10%. However the free radical complex produced from a high energy beam ($E_{beam} > 20$ MeV) and the way these radicals can effect the polarization is not yet well understood. For now we focus only on the ionization energy loss produced by the multi-GeV photon beam as e^+/e^- pairs. The energy loss from these processes is approximately independent of beam energy and is estimated to be about 2 MeV g^{-1} cm^2.

For a photon intensity of 1.5×10^{12} equivalent photons per second it is necessary to use an evaporation refrigerator with ∼1 Watt cooling power in combination with a high polarization, high radiation resistant proton target material (NH_3). For electron beam experiments typically 100 nA is the maximum current on the target. The heat load in a 3 cm long target can be calculated for NH_3 with density 0.917 g/cm^3 leading to,

$$2[\mathrm{MeVcm}^2/\mathrm{g}](1.6 \times 10^{-13}[\mathrm{J/MeV}])6.25 \times 10^{11}[\mathrm{s}^-1](3[\mathrm{cm}])(0.917[\mathrm{g/cm}^3]).$$

Only about 60% of the ionization energy is actually deposited into the target, leading to about 0.33 Watts. Combined with the heat deposit from microwaves (0.5 W), used to dynamically polarize the target, the cooling power of the UVA/JLab evaporation fridge and pumping system is not saturated. However, cooling power is not the only concern. This heat load must be distributed throughout the target so that the target material beads are not over-heated on the material boundary so as to create local depolarization. To do this with electrons a beam rastering system can be used to distribute the beam over the surface of the target face. The slow raster that spirals out is combined with the faster raster system which distributes the beam in a 2 mm^2 square pattern. Our high intensity photon source is designed to use the fast raster system, however with out also some sort of slow rastering there would be significant depolarization in the region around the photon beam spot due to material interfacial thermal heating (ITH).

The ionizing radiation inside the target is the primary source of the $\dot{N}H_2$ fee radical but also the ITH. Using simulations with the previously mentioned photon flux and a 2 mm^2 beam profile leads to 25 nA of ionizing radiation at the exit of the target in an area of about 6 mm^2 (containing 90% of the ionizing particles). Taking this spatial distribution to hold the full 0.33 W heat load from the high intensity photon beam implies that about 100 target beads with an average radius of 1 mm hold all the heat. To calculate the effects

of this heat load on the local polarization we must first start with the heat equation for a volumetric heat source. This can be expressed as,

$$C_{p0}T^3\rho\frac{dT}{dt} = \dot{Q} - 3R_\alpha\frac{T^4 - T_B^4}{r_{bead}}. \tag{1}$$

Using the corresponding values, this equation can be solved with the initial condition $T(0) = 1K$. $\dot{Q}$ is the volumetric heat load per bead which is conservatively estimated to be 0.72 W/cm^3. Using the specific heat for NH_3 of $C_{p0} = 8.8 \times 10^{-}6$ J g^{-1} K^{-4}, with ammonia Kapitza resistance $R_\alpha = 1.43 \times 10^{-}2$ W cm^{-2} K^{-4}, with T_B as the liquid helium bath temperature (1 K), and T is the dynamic material boundary temperature. The solution to this relation gives the boundary temperature as a function of time and is shown in Fig 1.

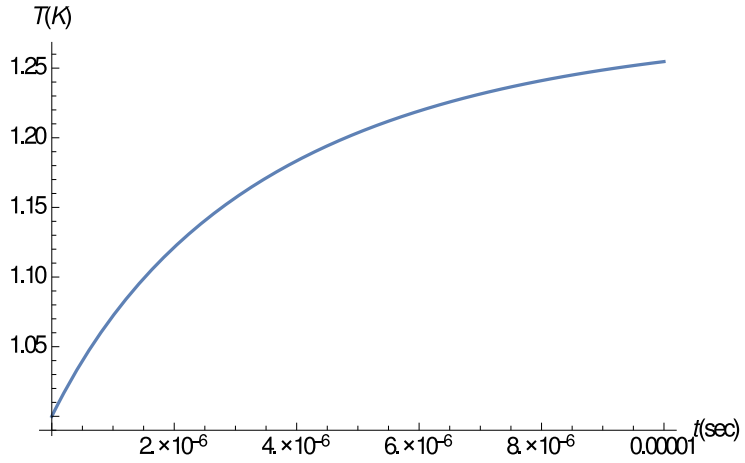

Figure 1. Ammonia bead temperature rise due to the beam heat load.

These results indicates that after a few microseconds the surface of the bead increases by about 0.25 K. We can then estimate the time it takes to heat the bead all the way through from the heat on the surface assuming spatial uniformity,

$$\Delta t = \frac{\rho V C_p \Delta T}{\dot{Q}}. \tag{2}$$

This calculation results in a time of just a few μs to heat the entire bead from the outer surface. These times are small on the scale of the time it take for the polarization to change. To estimate the time it takes to drive the polarization down from the material beam heating we must consider the DNP rate parameters of NH_3. This decay time is related to the microwave power and the spin-lattice relaxation rate. The equations of motion that give the rate of depolarization can be approximated using the form,

$$\frac{dP(t)}{dt} = \beta T^4(P_{lim} - P(t)). \tag{3}$$

The polarization, limited by the new thermal conditions from Eq. 3, is contained in P_{lim}, which is an estimate based on the Brillouin function. The parameter β contains the rate

information and comes from polarization data. The starting polarization of 93% is used as an example. Solving Eq. 3 numerically results in an approximation of the polarization drop over time.

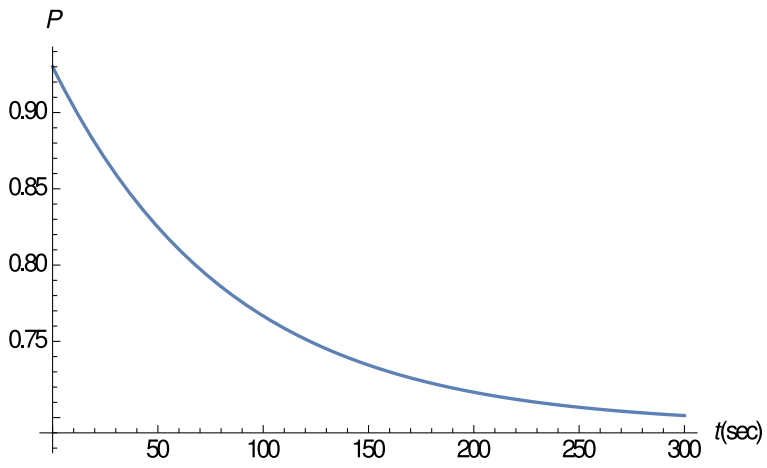

Figure 2. Rotating Target Cup

It is worth noting that calculations here are only estimates and several necessary parameters required have considerable uncertainty. We use the results as only a guide to give an order of magnitude check on the time need to rotate the target cell. Figure 2 indicates that the beads should only stay within the same position in the ionizing shower for no more than a few seconds or the polarization will decrease. This change would not register in the NMR signal. A rotation on the order of once every few seconds is adequate for this purpose.

The other demand on the target is, of course, the radiation damage induced by all forms of scattering in the target. If the dose that is mentioned previously (25 nA) from the ionizing radiation can be distributed over a standard target area of 570 mm^2, then the expected depolarization rate from radiation damage is still slower than that of an electron beam at 100 nA.

2 Design of Rotating Target

In order to increase the area of the target that the photon beam will interact with a rotating target was developed to raster photons over the target cup face, see Fig. 3. The Kel-F target cup is machined to include a gear that can be driven from a rotating shaft along the target insert. Fig. 3 shows a design of the same dimension of polarized targets used in the past (2.5 cm diameter by 3 cm length) that fit within the homogeneous field region of the polarizing 5 T magnet. In the design shown there is no additional material from the cup in the beam-line. The front and back of the target cell are made of a thin aluminum foil (not seen in the diagram). The rotation is driven by a gear and shaft. The NMR couples inductively to the target material by a coil wound around outside of the cup. The rotating shaft passes through the top of the target insert using a vacuum rotary feed-through which is then driven by a electric motor.

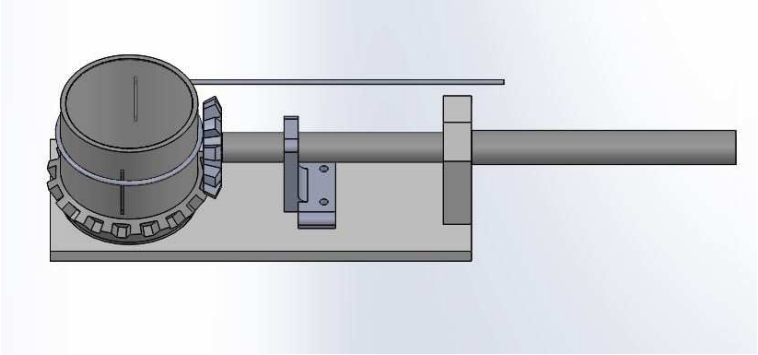

Figure 3. The rotating target cup driven by a gear and shaft with the NMR loop around the target cell.

The target rotation in combination with the standard target actuator results in an effective slow raster which spirals over the full area of the standard 2.5 cm diameter target. The beam collimation provides the spot size on the target and couples directly to the resolution characteristics for reconstruction at the cost of holding the beam location in space fixed. We can still obtain uniform exposure of the target cell by a combined rotation of the target cup synchronized with an up/down movement of the target ladder. Rotation of the target cup has already proven viable in many UVA tests. Depolarization and homogeneous radiation damage can easily be achieved by continuously moving the target at a rate determined by the radius of the circle made through rotation on the target surface, spending no more than a few hundred milliseconds on each target location. So even near the center only 0.01 Hz is required. To avoid mechanical vibration that can induce noise in the NMR signal it is possible to make several rotations in a fixed diameter before moving to the next actuator position. This reduces the up and down motion required to cover the same area. At UVA rotation rates of several Hz have already been demonstrated. By completing a fixed number of rotations for each experimental run, false asymmetries and fluctuations from the variations in target bead packing can be averaged out.

III The Compact Photon Source

A Conceptual Design

A traditional source of bremsstrahlung photons includes a radiator, a deflection magnet with large momentum acceptance, and a beam dump for the used electrons. Such a configuration requires significant space along the beam direction and heavy shielding due to the large openings in the magnet and the beam dump and the many meter length of the system. In addition, it leads to a large size of the photon beam at the target due to divergence of the photon beam and the long path from the radiator to the target. The beam spot size contributes to the angular and momentum reconstruction accuracies of the reaction products which experimentalists want to study. Lastly, it often comes with

appreciable radiation doses as particles are allowed to propagate over short distances before mitigation of radiation by containment starts. A new solution for a photon source was proposed in a report at the NPS collaboration meeting in November 2014 about a new experiment for a double polarized wide-angle Compton scattering from the proton at large (> 3 GeV^2) values of all three kinematical variables $s, -t, -u$.

The desirable size of the photon beam spot at the target is about 1 mm, which allows the scattered photon parameters to be reconstructed with an accuracy comparable to the proton arm angular resolution and the spacial resolution of the photon arm allowing the best selection of the exclusive WACS events. The design outlined in the 11/2014 report provides a photon beam spot with a diameter of 0.9 mm. However, the final experimental accuracy has several contributions, so even a 2 mm diameter spot is acceptable (see also a report [1]). This means that for an actual device we can use a distance between the radiator and the target significantly larger than the two meters presented in this document if it is needed in the engineering stage.

The concept of a new source takes advantage of the narrowness of the photon beam relative to the angular distribution of the secondary particles produced in the electron-nuclei shower. Indeed, the photon beam angular spread, dominated by an electron multiple scattering in the 10%X0 radiator, is about $4/E_{beam}$[MeV]$\sim$0.4 mrad, but the secondary particles survived filtering through a one nuclear interaction length ($\sim$140-190 g/cm^2 or $\sim$15 cm) of the heavy absorber, have an angular spread of 0.1-1 radian. The main elements of the CPS are shown in Fig. 4. Without loss of photon intensity, a channel (a

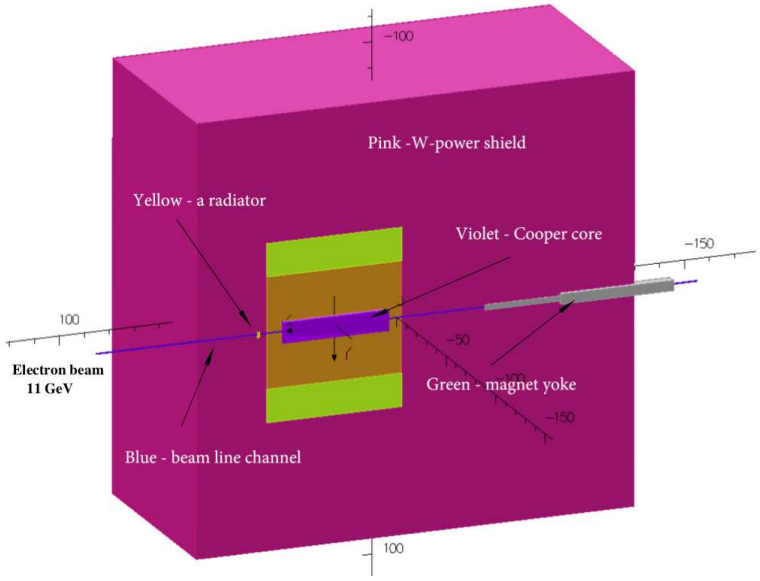

Figure 4. The CPS view.

collimator for the secondary radiation but not for the photon beam) around the photon beam could be as narrow as the photon beam size with natural divergence plus the size of the beam raster. After passing through the radiator, the electron beam should be removed from the photon line by means of a magnet. The length, aperture and field of the magnet are very different in the proposed source from the traditional one. In the

traditional source the magnet is needed to direct the used electrons to the dump. Because of the large momentum spread of used electrons, the magnet aperture needs to be big and the dump entrance should be even bigger (13% of the beam power would be lost before the beam dump, even with a 10% momentum acceptance of the beam line). In contrast, the proposed source has a dump inside the magnet.

The electron energy dumping starts on the side of the photon beam channel, so a shift of the electron trajectory by just 1-3 mm is already sufficient for the start of the shower. At the same time, such a deflection needs to be accomplished at a relatively short distance (much shorter than the size of the radiation shielding) after the beam passes through the radiator to keep the source really compact. Indeed, with a deflection radius, R, a vertical size of the channel, $2a$, and a vertical raster size, $2b$, the trajectory enters the channel side after traveling in the magnetic field the distance, p, which varies from $p = \sqrt{2\,R\,(a-b)}$ to $p = \sqrt{2\,R\,(a+b)}$ (see the scheme in Fig. 5). In the currently

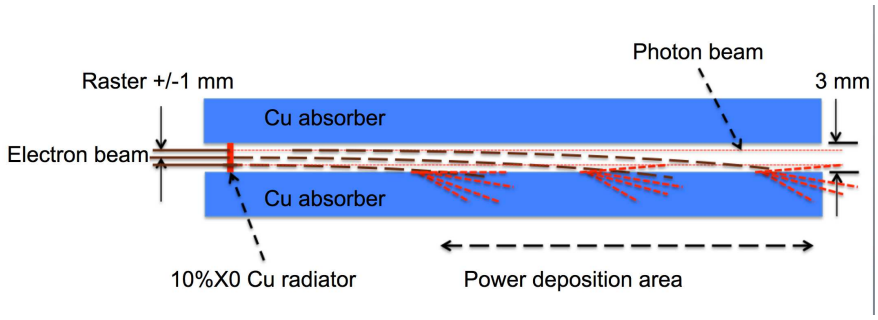

Figure 5. The scheme of beam deflection to the absorber/dump.

proposed CPS magnet the trajectory radius R is about 10 m for 11 GeV electrons, the channel size is 0.3 cm, and the raster size is 0.2 cm, so the distance p has an average value of 17 cm with a spread of 12 cm. A total field integral of 1000 kG-cm is adequate for our case. It requires a 50 cm long iron dominated magnet.

The above concept of the combined magnet-dump allows us to reduce dramatically the magnet aperture and length, as well as the weight of the radiation shield, due to the reduction of the radiation leak though the openings and the short length of the source. This consideration opens a practical way to CPS because it leads to a reduction of power deposition density in the copper absorber.

The WACS experiment will use a polarized proton target developed by UVa/JLab which reached very high parameters in terms of the proton polarization and beam intensity. The target has a large diameter of twenty millimeters, which is much larger than the desirable beam spot size. The beam degrades the target polarization very quickly if it stays at one location at the target. The traditional solution of such localized degradation of the target is fast movement of the beam spot, which allows avoiding overheating of the material and equalizing of the target degradation over the target volume. The beam raster, which moves the beam with a frequency of several Hz, was used in past experiments at Hall C. However, the CPS presented here has a very small aperture of 3 mm by 3 mm limiting possible beam motion. In the first CDR report [3], we proposed a scheme with several horizontal slots in the absorber and additional two mm vertical motion of the absorber which complicates its design.

An alternative approach for the beam-target raster proposed in the Ref. [2] includes a combination of the target rotation around the horizontal axis and ±10 mm vertical motion of the target ladder. Such a raster method effectively moves the motion complexity out of the high radiation area of the absorber. In case the proposed regular movement of the ladder (on the order of 10^6 cycles per experiment) is the subject of concern, we have a complementary solution for the vertical displacement of the beam spot. It could be achieved by a small variation of the vertical incident angle of the electron beam at the radiator. Indeed, with a ±5 mrad vertical angle variation and 200 cm distance between the radiator and the target, the displacement of the beam spot is equal to desirable ±1 cm. The required increase of the channel opening inside the CPS is about ±2.5 mm, which does not change the radiation confinement proposed in CPS.

B Magnet

Normal conducting magnets for high levels of radiation have been constructed at several hadron facilities, e.g. the neutron spallation source at ORNL and the proton complex JPARC. In fact, the radiation level expected in the source allows use of a modest cost kapton tape based insulation of the coils. We designed the magnet with permendur poles taped in two dimensions, which allows us to reach a strong magnetic field (3.2 Tesla) at the upstream end of the magnet, and moved the coils to 20+ cm from the source of radiation. The length of the magnet was selected to be 50 cm and the field integral 1000 kG-cm (see the field profile). Figure 6 shows the longitudinal profile of the magnetic field according to the OPERA calculation.

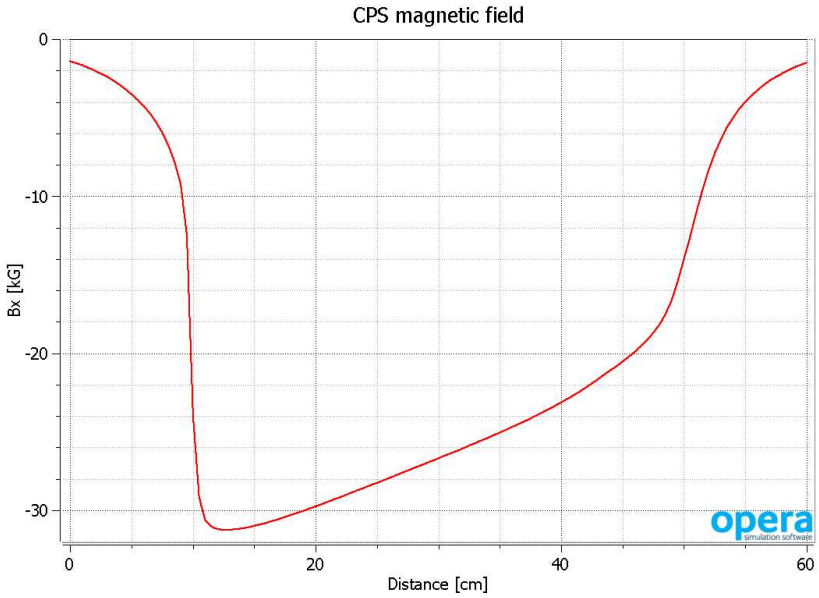

Figure 6. Magnetic field (B_x) profile along the beam direction.

C Central absorber

The beam power absorber will be made of copper, whose high heat conductivity helps to manage the power density. If it is needed, we can use an aluminum absorber, which would help to reduce power density even more by a factor of 2-3 due to a six times larger radiation length, but it would also increase the length of the source by about 50 cm. The heat removal from the copper absorber is arranged first via heat conductivity to the wider area where the water cooling tubes are located. At 10-15 cm from the beam line, the temperature of the copper insert drops to a level below 100°C (the calculation of the energy deposition was made in both the SIMC and Geant4 frameworks, and the temperature 2-dimensional analysis was performed for the highest power density area). Figure 7 shows the longitudinal profile of the power density according to the MC simulation.

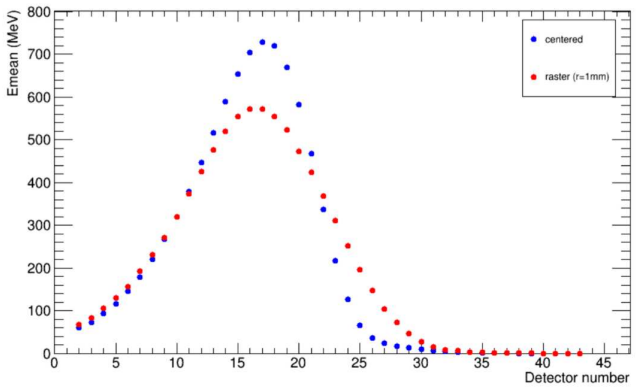

Figure 7. Longitudinal profile of the power distribution (integrated for one cm copper slab) for one 11 GeV incident electron. The maximum power density is at the coordinate 18 cm. The blue dots show the energy deposition for the electron beam centered in a 3 mm by 3 mm channel. The red dots show the same for the beam rastered with a radius of one mm.

The transverse distribution of power is also very important to take into account because, for a high energy incident beam, it has a narrow peak. A detailed MC simulation of power density and 2-dimentional heat flow analysis were performed to evaluate the maximum temperature in the copper absorber. Temperature was found to be below 400°C, which is well in the acceptable range for copper (the calculation was performed for the case of a 11 GeV 30 kW beam and a 10% X0 radiator). Figure 8 shows the temperature profile in the transverse plane at the longitudinal location of maximum power deposition. Cooling of the core will require about four gallons of water per minute at 110 psi pressure (at 30°C temperature rise), which is easy to provide.

D W-powder shield

The amount of material needed for radiation shielding is defined by the neutron attenuation length, which is 30 g/cm^2 (for neutrons with energy below 20 MeV) and 125 g/cm^2 (for high energy neutrons, see in PDG). The neutron production rate by an electron beam in copper is 1×10^{12} per kW of beam power according to the SLAC report

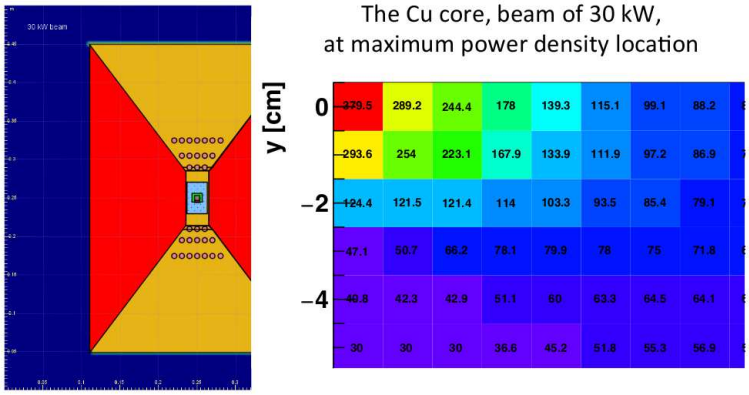

Figure 8. The cross section of the absorber (shown by yellow and blue in the center) with the cooling channels and the temperature map.

(W.P. Swanson, SLAC-PUB 2042, 1977, see Fig. 9). At a distance of 16 meters from the unshielded source for a 30 kW beam, the neutron flux would be 1×10^7 n/cm^2/s, which would produce a radiation level of 110 rem/h, or 850 times higher than during the RCS experiment (at a 16-meter distance from the pivot in the upstream direction). A radiation reduction factor of 1000 will be achieved by means of a shield with a mass of 850 g/cm^2. For the shield outside the magnet, the current design uses tungsten powder, whose high density (16.3 g/cm^3) helps to reduce the total weight of the device. A thickness of 50 cm was used as a first estimate for the thickness of the outer shield in CPS.

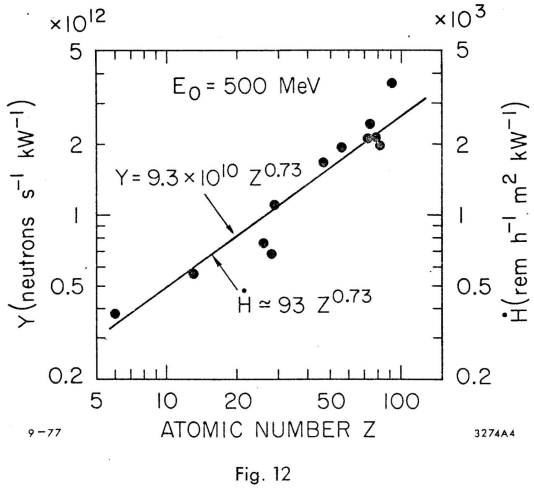

Figure 9. The neutron yield according to Swanson's report.

IV Radiation Requirements

The goal of the Compact Photon Source is to convert beam energies of up to 12 GeV with currents of up to 5 μA into a high-intensity source of collimated photons. For the Hall-D adaptation, the 5 μA beam current is limited by the design of the Hall D Tagger Magnet alcove. This corresponds to a 60 kW power limit. For the Halls A/C adaptation, the beam energy is limited to 11 GeV. Many experiments will opt to use the traditional method for photon beam experiments, with the high-current electron beam striking a 10% radiation length Cu radiator. The Compact Photon Sources gain in Halls A/C is foreseen for use with Dynamically Nuclear Polarized targets. Electron beam currents for use with such targets is typically limited to 100 nA or less, to reduce heat loading and radiation damage effects. The equivalent heat load for a pure photon beam impinging such targets corresponds to a photon flux originating from a 2.7 μA electron beam current striking a 10% Cu radiator. Hence, the Compact Photon Source design for Halls A/C should be able to absorb 30 kW in total (corresponding to 11 GeV beam energy and 2.7 μA beam current).

In addition, the typical beam time we assume for an approved experiment at Jefferson Lab is 1000 hours ($\approx$40 PAC days). For such a Compact Photon Source experiment, one needs to fulfill the following radiation requirements:

- Prompt dose rate in hall $\leq$ several rem/h at 30 feet from device.
- Prompt dose rate at the site boundary $\leq$ 1 μrem/r (2.4 μrem/h corresponds to a typical experiment at Jefferson Lab not requiring extra shielding).
- Activation dose outside the device envelope at one foot distance is $\leq$ several mrem/h after one hour following the end of a 1000 hour run.
- Activation dose at the pivot in the experimental target area, where operational maintenance tasks may be required, is dominated by the dose induced by a pure photon beam, and at one foot distance from the scattering chamber $\leq$ several mrem/h after one hour following the end of a 1000 hour run. *i.e.*, the additional dose induced by radiation of the main beam absorbed in the Compact Photon Source is negligible.

The Compact Photon Source design should combine in a single properly shielded assembly all elements necessary for the production of the intense photon beam, including that the operational radiation dose rates around it are acceptable as outlined in the requirements above. Much of this is achieved by keeping the overall dimensions of the setup limited, and by shielding induced radiation doses as close to the source as possible, and by careful choice of materials. Compared to the traditional bremsstrahlung photon source, the proposed solution will present several advantages, including much lower radiation levels, both prompt and post-operational due to the beam line elements radio-activation, as will be shown later.

The Compact Photon Source conceptual design has been established with extensive and realistic simulations. As validation of the simulation tools used, we have also performed a benchmark comparison using tools such as GEANT3, GEANT4, FLUKA and

DINREG. The benchmark results are further described in Appendix B. After benchmark validation, we have performed an extensive series of radiation calculations to:

- Determine the size and layering of the shielding around the magnet, and the choice of materials (Cu, Cu-W alloy, concrete, borated plastic, etc.).
- Determine the magnet field requirements in terms of peak field, gap size, and field length.
- Determine the radiation level on the magnet coils and based on these results identify radiation hardened materials that might be used in building the coils.
- Determine the radiation level on the polarized target electronics.
- Determine the radiation level immediately next to the device as well as at the experimental hall boundary.

The logic behind the CPS hermetic shielding design is that radiation (γ, n) from the source should be a few times less than from a photon beam interaction with the material of a polarized target. The CPS is designed to meet the accpetable radiation level requirements specified in Appendix 2 for electron beam current of 2.7μA (30 kW), run time of 1000 hours, and the photon source as close to the target as possible. The shielding design consists of tungsten powder and 10cm of 30% borated plastic. The addition of the latter has considerable impact in reducing the neutron flux, illustrated in Figure 13.

V Radiation Studies and Shielding Design

In this Section we will describe several different configurations for comparison. One is what has been the default situation for Dynamically Nuclear Polarized targets in Hall C and elsewhere, assuming an up to 100 nA electron beam current we call this scenario "100 nA electron beam". A second configuration is the equivalent photon flux created by a 2.7 μA electron beam on a 10% Cu radiator, impingent on the same polarized target system. Here, we removed all the secondary particles generated, so this situation mimics a pure and background-free photon beam. This scenario is called "2.7 μA photon beam". The third scenario is that with the CPS (Compact Photon Source), under the same conditions: a 2.7 μA electron beam strikes a 10% Cu radiator. Here, all the radiation background is taken into account and simulated. In some cases we have simulated only the effect of the CPS, in some cases the CPS and the target system combined. These scenarios are called "CPS", or "CPS with Polarized Target".

1 Prompt Radiation Doses (without a Target)

To explain the shielding concept of the CPS, we start with comparing the prompt radiation doses as calculated in a ring detector which covers a range between 5 and 10

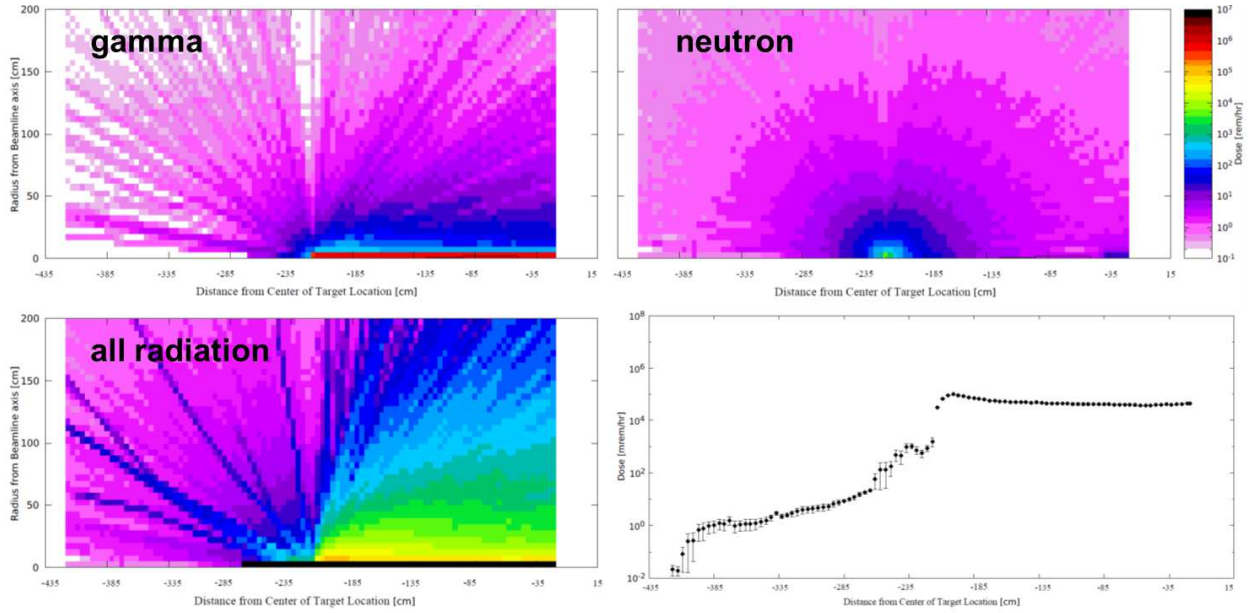

Figure 10. Two-dimensional dose rates as originating from photons only (top left), from neutrons only (top right), from all particles (bottom left) and the (one-dimensional) prompt radiation dose along the beam direction (bottom right).

cm radius from the beam line. This such that we could directly compare GEANT and FLUKA calculations.

We first calculate the prompt doses originating from a 2.7 μA electron beam hitting a 10% Cu radiator a distance of 2.15 meter before the pivot. There is no target system in this simulation, and all prompt radiation originates from the Cu radiator. Figure 10 shows two-dimensional dose rates as originating from photons only (top left), from neutrons only (top right), from all particles (bottom left) and the (one-dimensional) prompt radiation dose along the beam direction (bottom right). Obviously, most prompt radiation is created along the beam direction, although this is less obvious from the neutron-only figure. The prompt radiation levels reach roughly 40 rem/hour. Interestingly, the gamma-only contribution only amounts to roughly 200 mrem/hour, and the neutron-only is less than 10 mrem/hour. They together fail to account for the total prompt radiation simulated along the beam line. That there is another contribution can readily be seen from the bottom right panel, which shows another source of prompt radiation coming in these are the charged electrons and positrons created, inducing further showers.

A striking difference is observed for the same situation, a 2.7 μA electron beam hitting a 10% Cu radiator, but now within the CPS. Figure 11 illustrates the prompt radiation dose along the beam direction. The scales of this Figure are consistent with those in Figure 10 (bottom right panel). One can see the prompt radiation (again, in a 5 to 10 cm ring detector along the beam axis) within the CPS is much higher, but outside the CPS the prompt radiation dose is reduced to roughly 15 mrem/hour, a reduction by over a factor of 1000! This factor is entirely consistent with the predicted radiation reduction factor of Section III D.

Why this magic? This is further illustrated in Figure 12. In the first three panels

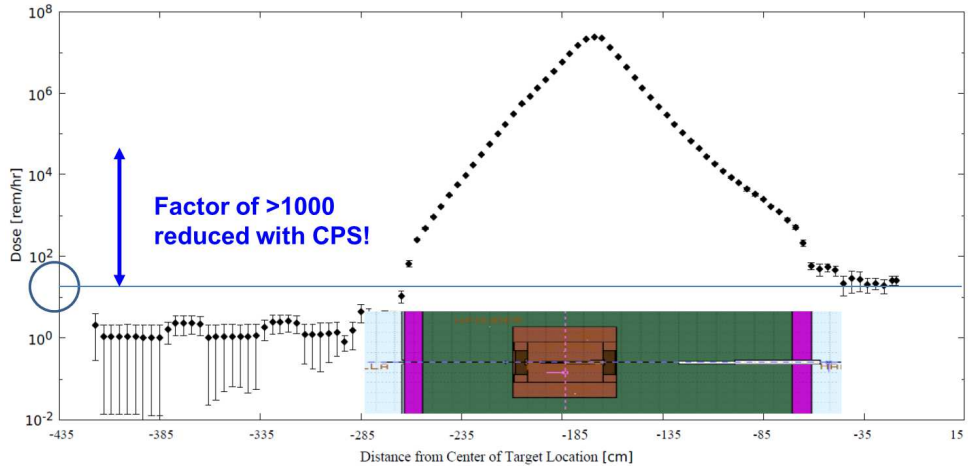

Figure 11. Two-dimensional dose rates as originating from photons only (top left), from neutrons only (top right), from all particles (bottom left) and the (one-dimensional) prompt radiation dose along the beam direction (bottom right)..

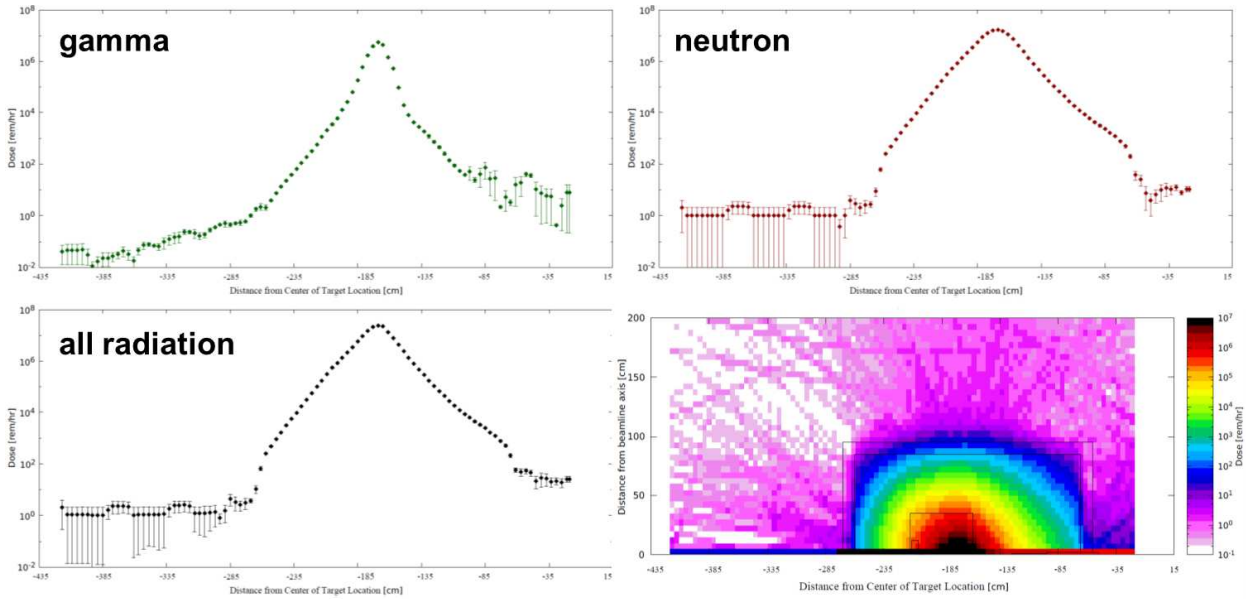

Figure 12. The (one-dimensional) prompt radiation rates as originating from photons only (top left), from neutrons only (top right), and from all radiation sources (bottom left). The fourth panel (bottom right) illustrates how well an optimized CPS shielding concept absorbs the prompt radiation, outside the CPS the prompt radiation is on the surface (indicated by the outer black rectangular lines) already reduced to a level of roughly 10 rem/hour at most.

we show the (one-dimensional) prompt radiation rates as originating from photons only (top left), from neutrons only (top right), and from all radiation sources (bottom left). In striking contrast with the case without CPS, there is no contribution from photons, electrons, and positrons anymore: the neutron-only calculation is near-identical to the all-radiation-calculation. The fourth panel, Figure 12 (bottom right) illustrates how well

an optimized CPS shielding concept absorbs the prompt radiation, outside the CPS the prompt radiation is on the surface (indicated by the outer black rectangular lines) already reduced to a level of roughly 10 rem/hour at most. The shielding concept works so well as showers never get a chance to develop and photons are contained. There will always neutrons leak out.

This indirectly confirms that with a CPS the prompt dose rates in the hall can easily obey the following requirement: **Prompt dose rate in hall $\leq$ several rem/h at 30 feet from device**.

2 Impact of Boron and Shielding Optimization

It is well known that the neutron fluences can be drastically reduced by the addition of boron, which acts as an excellent capture material for low-energy neutrons. We simulated this property ourselves by calculating the neutron flux at the CPS boundary assuming various thicknesses of tungsten shielding (65, 75 and 85 cm radial), and then adding 10 cm of borated (30%) plastic. The result can be seen in Figure 13, showing the neutron flux as function of neutron energy (on a logarithmic scale). Adding 10 cm of tungsten reduces the neutron flux, but a much more drastic reduction is seen when adding the 10 cm of borated plastic. Thus, in our design we assume an outer layer of the CPS, beyond the tungsten powder, of borated plastic with a thickness of 10 cm.

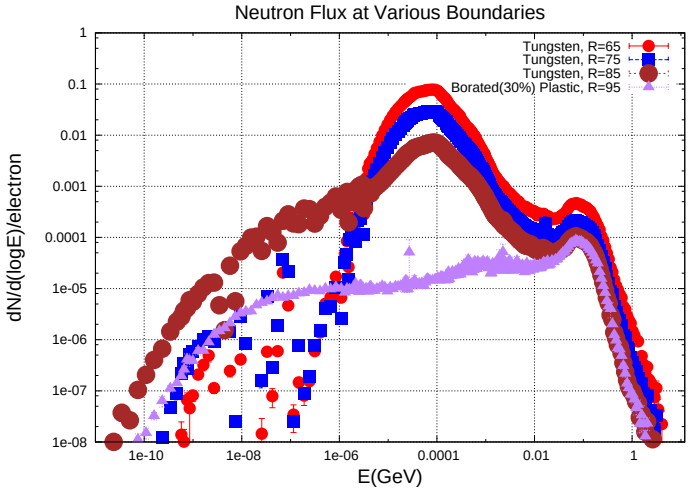

Figure 13. Impact of boron on shielding properties.

That our shielding design has been optimized well can be further exemplified in Figure 14. In the right panel we show the prompt radiation rates with the optimized shielding design, whereas in the left panel we show the same prompt radiation rates if we would have had 10 cm less of tungsten shielding, and no borated plastic. The effect is remarkable, one readily can witness much higher prompt radiation rates escaping the CPS. But this also shows our CPS shielding design is well optimized! Please do note that in these panels the CPS magnet is assumed to be at the center (zero distance) along the beam line, in contrast with earlier Figures.

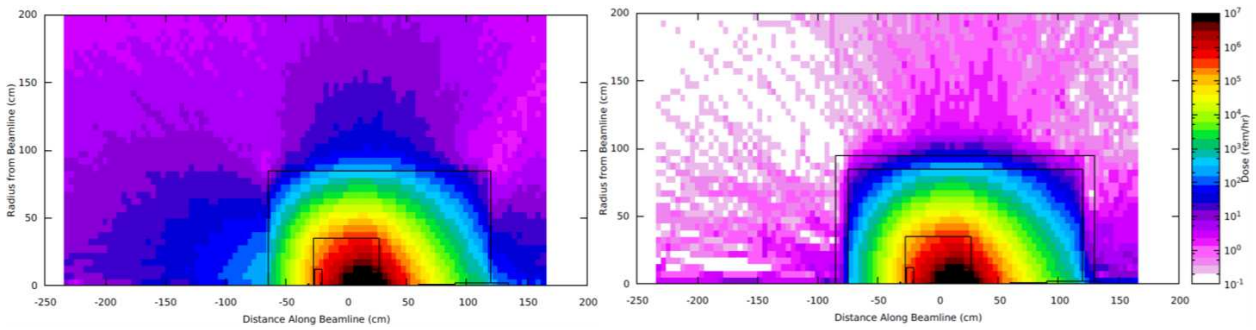

Figure 14. The prompt radiation rates with the optimized shielding design, whereas in the left panel we show the same prompt radiation rates without extra shielding (10 cm less of tungsten shielding, and no borated plastic). Note: these are with the CPS magnet centered around "zero" along the beam line.

3 Prompt Dose Rates at the Boundary

In benchmark calculations assuming spheres of pure shielding materials (see a more extensive description of the benchmark calculations in Appendix VI B 10) we find that the prompt dose rate estimates at the RBM-3 boundary are 0.24 μrem/hour for a 3 meter (diameter) iron sphere and 2.4 μR/hour for a 1.5 meter (diameter) tungsten sphere.

Our typical CPS shielding is assumed to be 85 cm thick radially and surrounded by 10 cm or borated plastic. Hence, the boundary dose is tuned below the 2.4 μrem/hour that corresponds to a typical experimental run at Jefferson Lab not requiring local shielding per the radiation budget. So, we are already **below the level of 2.4 μrem/h corresponds to a typical experiment at Jefferson Lab not requiring extra shielding**. With further choice of proper material and ordering, the boundary dose can be tuned even further down, as required.

We do note that for Hall D the CPS design is compatible with the site boundary as the conditions for the regular Hall D tagger magnet operation can dump up to 60 kW in a local beam dump: the Hall D tagger building has been designed assuming an up to 12 GeV beam energy and an up to 5 μA electron beam current. For the CPS, one can thus assume the Hall D tagger magnet building shielding is appropriate also when up to 60 kW is dumped in the CPS itself. Additional local shielding may be required.

4 Activation Doses (without a Target)

We now turn to the activation doses expected around the CPS. Figure 15 shows the calculated activation dose one hour after a 1000-hour experiment under the described conditions (2.7 μA, 10% Cu radiator, with shielded CPS) has been completed. Please note again that in this Figure the CPS magnet is assumed to be at the center (zero distance) along the beam line. The radiation calculations show the activation dose outside the CPS is reduced to the order of roughly 1 mrem/hour. To quantify this further, Figure 16 shows the activation dose radially away from the CPS. The activation dose outside the CPS is, one hour after a 1000-hour run, reduced to 2 mrem/hour on contact and reduces radially

outward. At one-foot distance, it is reduced to about 1.5 mrem/hour, and at two-feet distance to less than 1 mrem/hour.

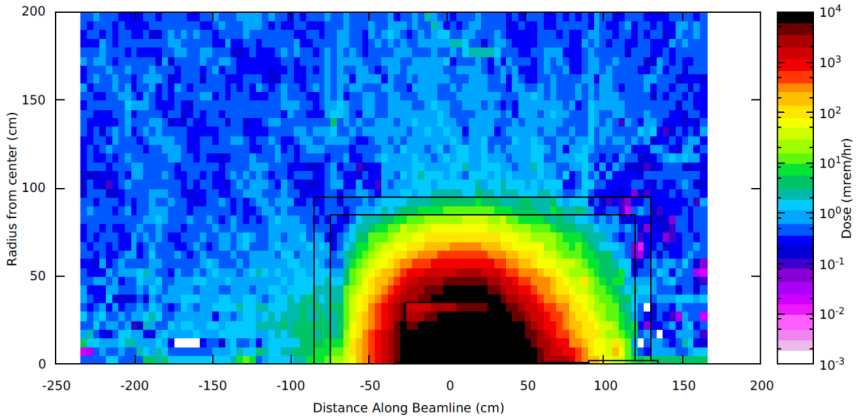

Figure 15. Calculated activation dose one hour after a 1000-hour experiment under the described conditions (2.7 μA, 10% Cu radiator, with shielded CPS) has been completed. Note: these are with the CPS magnet centered around "zero" along the beam line.

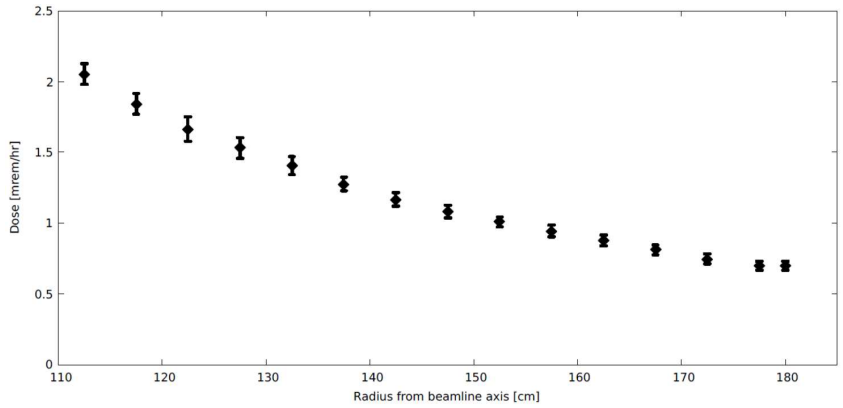

Figure 16. Activation dose outside CPS 1 hour after a 1000 hour run is 2 mr/hr on contact and reduced radially outwards.

Hence, this easily fulfills the requirement that **Activation dose outside the device envelope at one foot distance is $\leq$ several mrem/h after one hour following the end of a 1000 hour run.**

Note that these estimates do not depend much on the assumed 1000-hour continuous run, we also simulated a 100-hour continuous run but the activation doses are, albeit slightly smaller, nearly the same, reflecting that much of the activation is instant. Activation doses also do not drop appreciably drop if one waits one hour or one day. On the other hand, if one would wait a week or a month the activation doses at contact can be reduced by up to a factor of ten. Inside the CPS, the activation doses can be up to 1 Krem/hour, which is why we will move the CPS laterally to the side in between experiments, with rails on a stand, and do not disassemble.

5 Radiation Doses with a Target

In the further radiation calculations, we have also included the polarized target scattering chamber and target system. In Figure 17 we illustrate our setup and show a side view of the Compact Photon Source, indicating the magnet, the W powder shield, and the layer of borated plastic, and also the scattering chamber with polarized target system. The description of the scattering chamber and polarized target includes: (i) the exact diameter of the scattering chamber and all the ports with their exact dimensions and window materials, and (ii) the polarized target material but also the liquid helium surrounding the target beads, etc.

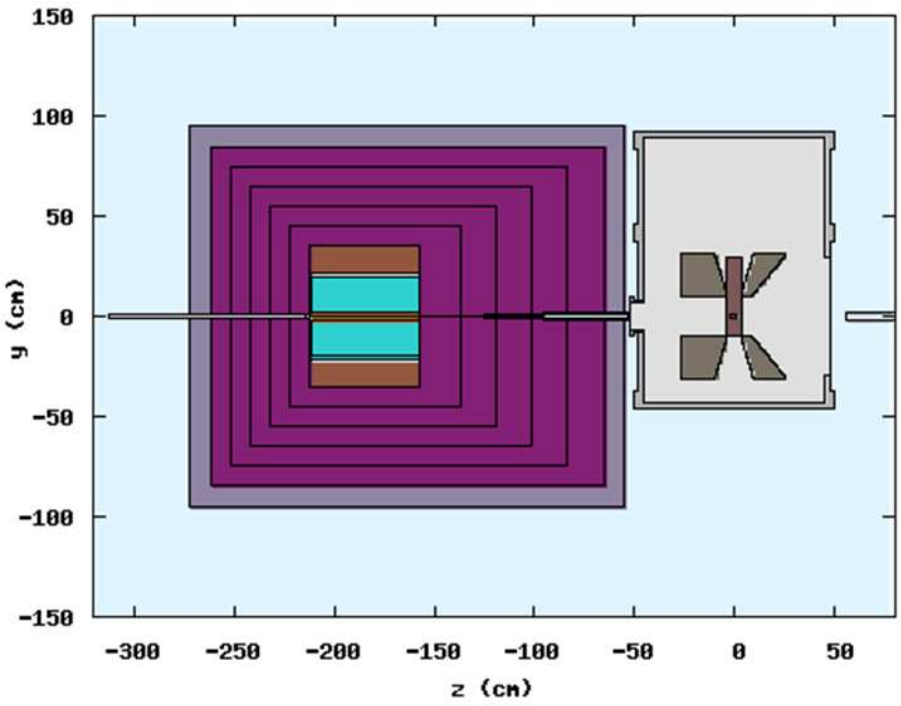

Figure 17. Side view of the Compact Photon Source, indicating the magnet, the W powder shield, and the layer of borated plastic, and also the scattering chamber with polarized target system.

We add Figure 18 for completeness, it illustrates the 1-MeV neutron equivalent damage to silicon (in neutrons/cm^2). This is the relevant quantity to use to outline when one has to worry about radiation damage to sensitive electronics. The result, not surprisingly, shows that there is a narrow cone in the forward direction, along the beam axis, up to roughly one meter, that should be evaded for electronics.

Figure 19 shows the prompt dose at the target for different configurations. The distance R is radial distance from the pivot, with the radius of the scattering chamber boundary at 50 cm. The various calculations reflect the "100 nA electron beam" (red downward triangles), the "2.7 μA photon beam" (blue upward triangles), the "CPS" (without polarized target, black circles), and the "CPS with Polarized Target" (mauve squares). At the boundary of the scattering chamber, the "100 nA electron beam" con-

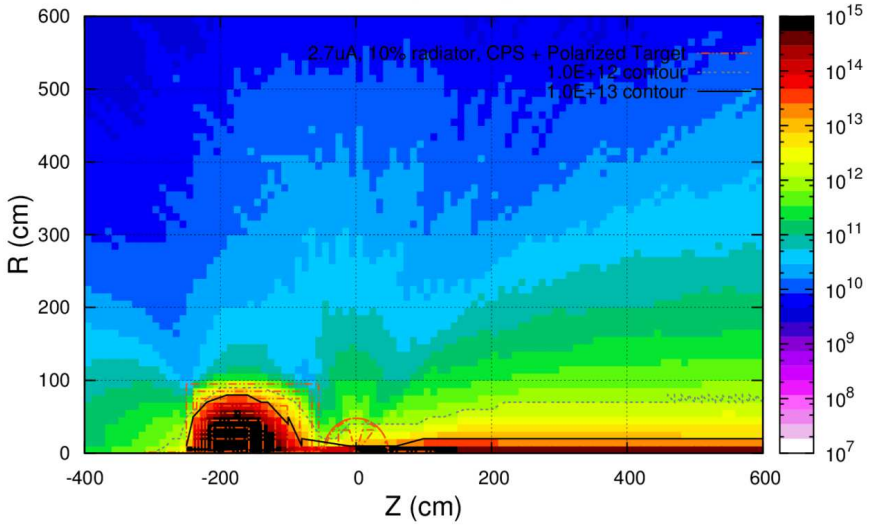

Figure 18. 1-MeV neutron equivalent damage to silicon (in neutrons/cm^2).

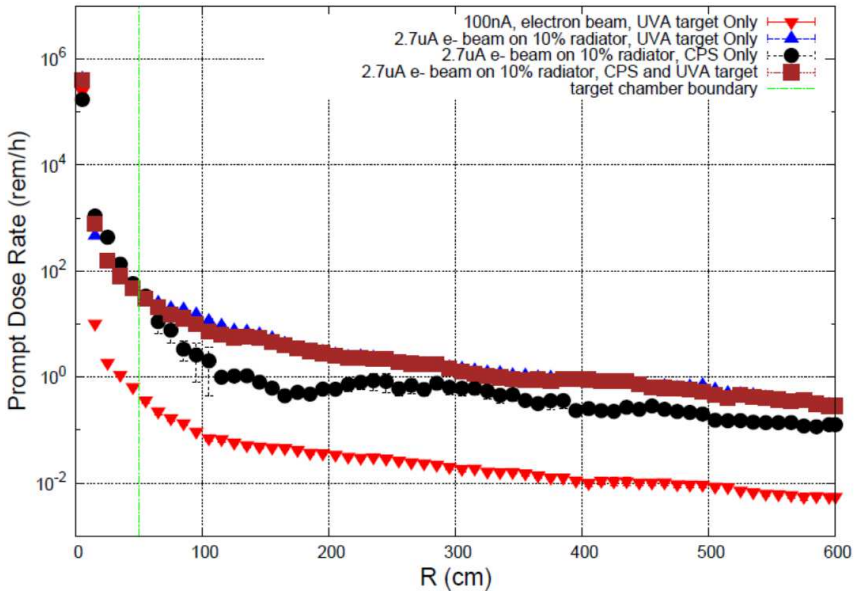

Figure 19. Prompt dose at the target for different configurations. Distance R is radial distance from the pivot, with the radius of the scattering chamber boundary at 50 cm.

figuration, the default operating mode for polarized beam experiments with dynamically nuclear polarized targets to date in Hall C, the prompt dose is roughly 1 rem/hour. The "2.7 μA photon beam" scenario is roughly 30 rem/hour. This simply reflects that even if a 2.7 μA pure photon beam deposits the same heat load in a target as a 100 nA electron beam, the radiation rate is much higher. The "CPS with Polarized Target" scenario is identical to the pure photon beam. Hence, no additional radiation comes from the CPS, it is well shielded.

Figure 20 is perhaps more instructional, in that it shows the activation dose rates

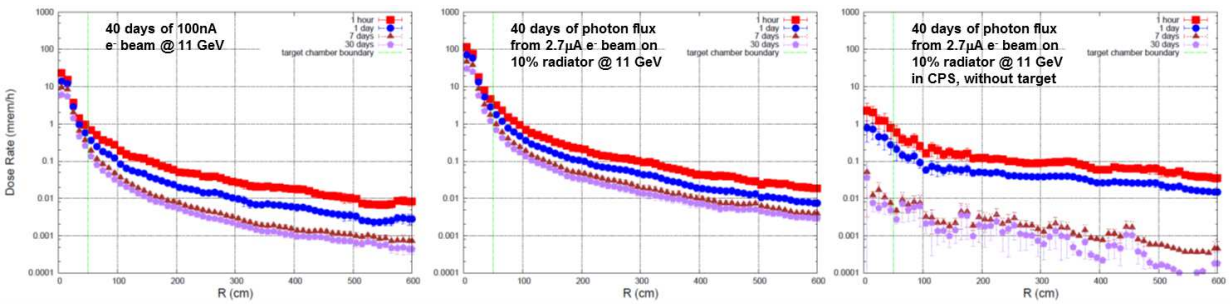

Figure 20. Activation dose rates at the target for different configurations. Distance R is radial distance from the pivot, with the radius of the scattering chamber boundary at 50 cm.

for three configurations, "100 nA electron beam" (left), "2.7 μA photon beam" (middle), and "CPS" (without polarized target, right). The figure panels have different vertical size, such that equal dose rates line up from left to right. One directly can see that the "2.7 μA photon beam" configuration has much higher activation doses than the "100 nA electron beam". This again reflects what was seen in Figure 19 also for prompt radiation dose rates, there are a large amount of more photons coming from a 2.7 μA electron beam on a 10% Cu (radiator) target than there are from a 100 nA electron beam on a roughly 3% dynamically nuclear polarized target (we assumed NH3). More interestingly, the effect of the CPS is negligible: activation near the target does not come from the CPS itself, it rather comes from the powerful photon beam we have created. The price to pay is that one ends up with a roughly constant 0.1 mrem/hour activation level at large radial distances, but this is negligible.

We also indicate in the various panels how fast the activation decays, and indicate levels after 1 hour, 1 day, 1 week, and 1 month. One can see that the 0.1 mem/hour activation level one has induced by the use of the CPS has a long life-time but has decayed away after a week. This is consistent with what was observed in the example of the activation levels at radial distances around the CPS above.

Lastly, we illustrate in Figure 21 in a two-dimensional plot the activation dose rates one hour after a 1000 hour run with the Compact Photon Source, with a 2.7 μA beam and a 10% radiator and an 11-GeV electron beam energy, and the polarized target system (at z = 0). The 1 mrem/hour contour is indicated.

This proves that with the well-shielded CPS design, the **Activation dose at the pivot in the experimental target area, where operational maintenance tasks may be required, is dominated by the dose induced by a pure photon beam and is at one-foot distance from the scattering chamber $\leq$ several mrem/h after one hour following the end of a 1000 hour run**, and also that **the additional dose induced by radiation of the main beam absorbed in the Compact Photon Source is negligible**. This was the last of the radiation requirements put forward in Section IV.

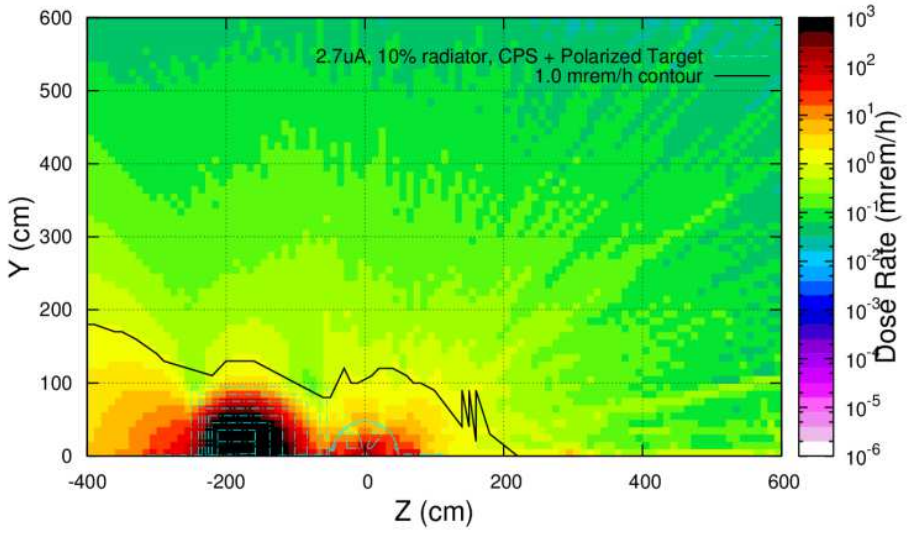

Figure 21. Activation dose rates one hour after a 1000 hour run with the Compact Photon Source, a 2.7 μA beam and a 10% radiator, at 11 GeV beam energy, and the polarized target system (at $z = 0$). The 1 mr/hr contour is indicated.

VI Safety and Engineering Aspects

A Safety

Realization of the proposed device will boost the experiment productivity by a factor of 30 but it is relatively expensive and require especially reliable construction methods. From safety point of view the CPS device is a modest power (30 kW) beam dump installed in a middle of the hall. There are several safety aspects in this project. Here we show a list for a full scope including items which are already analyzed in the previous sections of this document and a few others which will be considered in detailes in future stages of development.

- Prompt radiation level in the hall
- Radiation level at the JLab boundary
- Residual radiation in the hall
- Radiation level at the polarized target coils (both prompt and residual)
- Radiation level at the detector electronics
- Radiation level at the magnet coils and absorber cooling water
- Radiation aspects after experiment completion
- Safety documentation, review, and approvals

The current results are based on the studies of the radiation levels using FLUKA (also comparison with Geant4) and comparison with the data from several experiments already performed at JLab. Regarding first two items we found that levels of radiation is well below typical for high luminosity experiments in Hall C or A. The residual radiation on the surface of CPS is of a few mrem/h after 100 hours cooling. Radiation on the CPS magnet coils was found to be of 80 kRad/h, see Ref. [3], page 19. Prompt radiation level on the polarized target coils is about 150 rem/h due to interaction of the photon beam with the material of the polarized target.

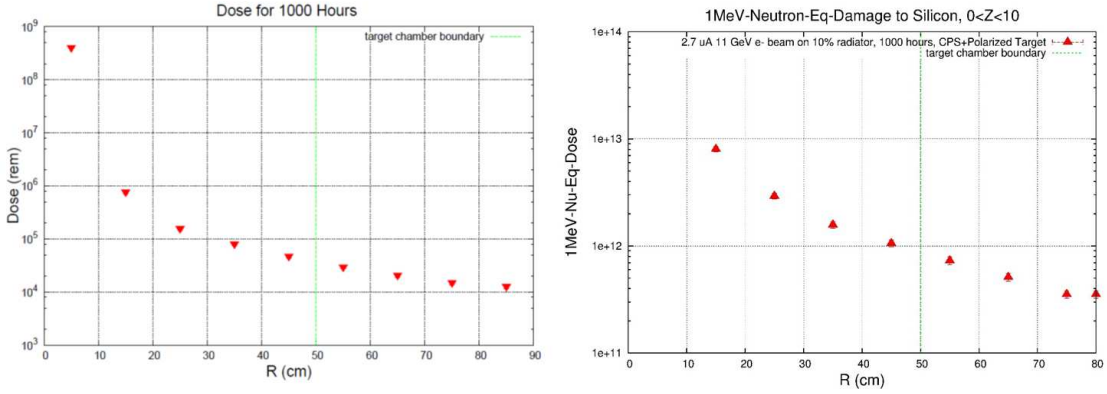

Figure 22. The prompt dose rates (right) and the resulting 1 MeV neutron equivalent damage to silicon (left) in the target area, assuming a 1000 hour run with the Compact Photon Source with a 2.7 mA beam, a 10% Cu radiator, and 11 GeV beam energy. The polarized target system is at z = 0 and the nominal target chamber radius is 50 cm. The target coils are at about 20 cm from the beam line. The dose for 1000 hours of beam time at the target coils is 5 times 105 rem and the 1 MeV neutron equivalent damage is 5 times 1012 neutrons/cm2. The contribution of the CPS backgrounds to these numbers is negligible (contributing 2.5% only).

B Engineering

The CPS device is a specialized beam dump but many considerations for the design are similar to the medium power dumps constructed at Jefferson Lab, see e.g. Ref. [4]. In addition to the radiation and power handling considerations we need to take into account short term nature of CPS installation for just one or several experiments, which requires removal of the activated system from the beam line soon after experiment completion.

The CPS is planned to be installed 5 meters upstream of the hall pivot and the polarized target 7 meters from usual location because the experiment does not use SHMS/HMS but both detector arms (NPS and BigBite) will have custom support frames. The NPS and Bigbite will be located on the floor between SHMS and HMS as close as feasible to the present Hall C Pivot.

The CPS will be installed in the area upstream of the Hall C pivot which is already occupied by several Hall C systems. The final Hall C girder containing BPMs, BCMs, correctors and other devices will have to be significantly modified. The cost for this modification and remount of the instrumentation must be estimated and included in the

experiment total. The downstream portion of this girder is cantilevered over the SHMS data cable hoses which arc around the pivot and permit rotation. The SHMS Data hoses cannot be removed or significantly modified. They do permit legs for the CPS stand. These legs may limit the freedom of SHMS rotation somewhat.

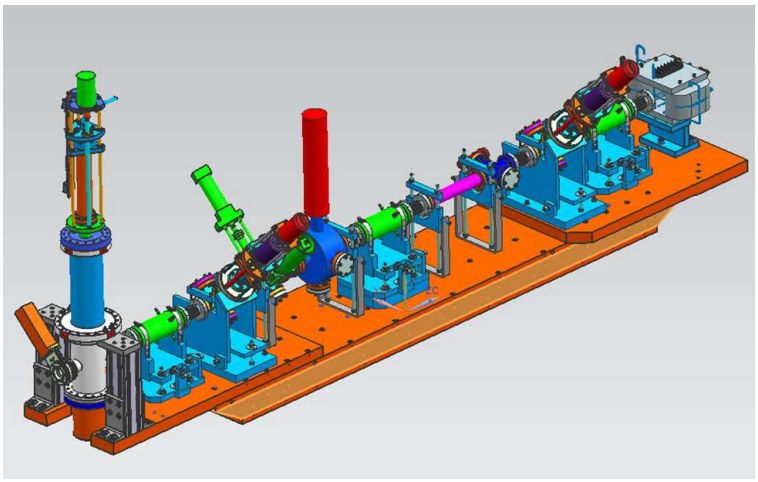

Figure 23. The present final girder in Hall C.

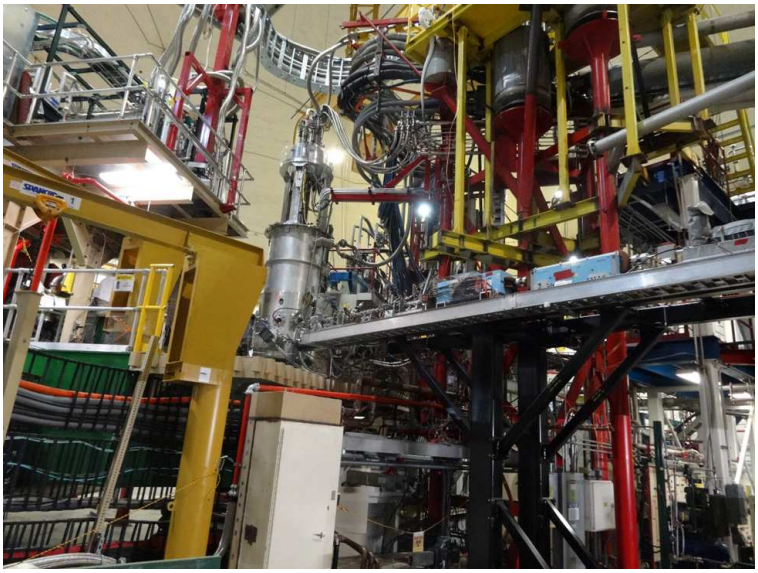

Figure 24. Final Hall C girder, SHMS data cable hoses and environment.

There were considered the following engineering aspects in the CPS project:

- Forces from the closely located magnets
- Modification and rebuild of the Hall C final instrumentation girder
- Installation/survey of CPS on the beam line

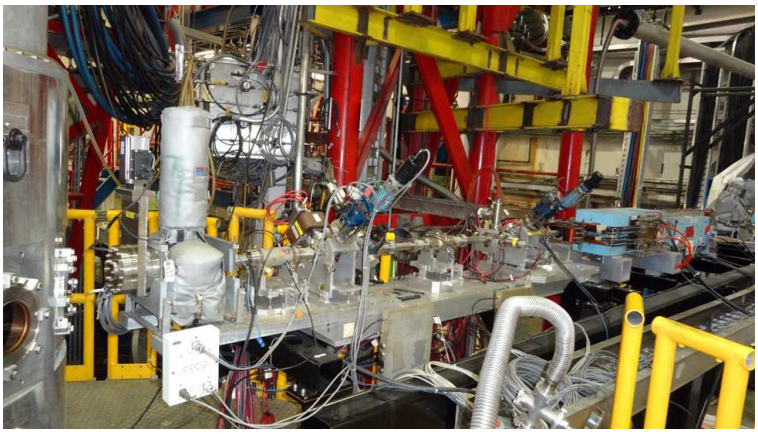

Figure 25. Closer view on final Hall C girder.

- Fast raster trip detection and raster interlock
- Interlock system: temperatures, radiation, water flow
- Commissioning plan including some engineering tests
- Removal of the CPS from the beam line after the experiment
- Safety documentation, review, and approvals
- Preliminary cost estimate

1 Magnetic Forces and Gradients at the Polarized Target

The CPS magnet will be located relatively close to the 5 Tesla solenoid of the polarized target whose mutual forces need to be taken into account in the design of the support structure and may require compensation. Preliminary analysis was already performed in the technical note in 2015 for iron-based shielding which currently replaced by W-power which reduced forces very much. Residual fields and forces form the CPS magnet will require iron shielding to avoid interference with the Polarized Target magnet. Another magnetic consideration is the effect on field quality at the polarized target. The fields and gradients imposed on the Polarized target will not be large but they must be compensated at the 10^{-4} level. Some magneto-static effort to model the target environment and design a compensation system is required.

2 Pre-Assembly and Fiducialization of the CPS

The CPS should be pre-assembled in the Test Lab. During assembly and after completion the CPS can be measured and fiducialized to facilitate final alignment in Hall C. Progressive measurement and fiducialization will eliminate problems with position references becoming hidden. Transporting the CPS to hall C in one piece will preserve

the alignment and avoids introduction of errors due to dis-assembly and re-assembly. This would require a large crane in Hall C but no dis-assembly/re-assembly is required so it is likely to be the cheaper alternative. A comprehensive set of safety and operational test can be performed once CPS is assembled (see safety section following). to the movable platform (on the rollers) after experiment. Then the source will be stored in the hall until activation is sufficiently low for opening the shield.

3 Installation Considerations in Hall C

Installation of the CPS in Hall C will consist of the following steps:

- Removal of the Final Girder
- Remote girder dis-assembly and remount of instrumentation on the new girder
- Presurvey for mounting of the CPS stand.
- Mount CPS stand to Hall C floor
- Transport and Crane in complete CPS using a 150 Ton truck crane
- Survey and alignment of CPS
- Installation of new girder and instrumentation
- Survey and alignment of new girder
- Connect CPS magnet power and water and test
- Connect new girder and test
- Restore beam vacuum in Hall C

The CPS installation scheme is shown in Fig. 26.

4 Interlocks, Instrumentation and Controls

The CPS should be heavily instrumented for early detection of problems such as low coolant flow, leaks, low pressure, high temperature, high conductivity etc. The protection and safety of the CPS begins with the design which must err on the side of conservatism especially in the magnet coil design and dump cooling. A very low current density design is suggested not to exceed 500 Amps/cm^2. Individual coil pancakes leads should be extended to an area outside of the magnet and shielding for easy access. There should be NO electrical or coolant joints inside the CPS shielding. Every separate sub coil of the CPS magnet should have thermometry, klixons and flow measurements to avoid any possibility that one of the separate current paths can overheat due to being starved of coolant, a leak or a bad electrical joint. Voltage monitoring of each sub coil is cheap insurance against overheating from any source including , internal blockage, leaks, flow

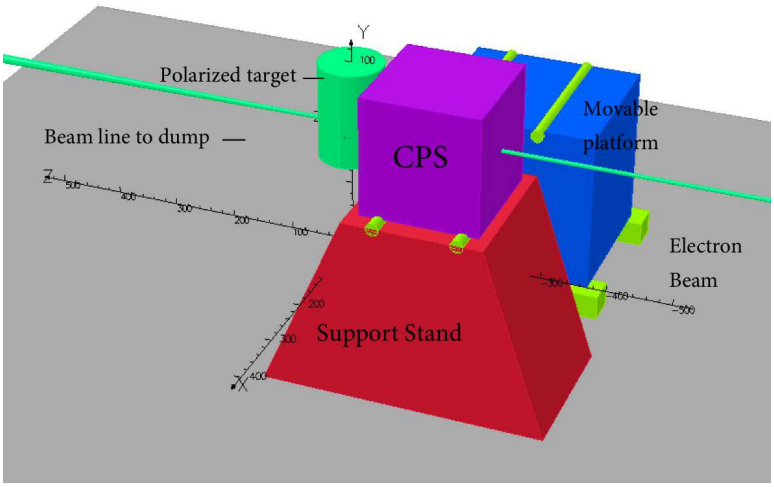

Figure 26. The CPS view in the hall. The electron beam is going from the right to the left. The movable platform (shown as a blue box) has two rails shown as green cylinders.

restrictions or bad electrical connections. Extra insulation between sub coils and between the coil and ground can prevent ground faults. A commercial power supply is assumed and these come with a wide array of internal interlock protections. The available interlocks and signals would eb fed into the FSD system to prevent damage.

5 Fast raster trip detection and raster interlocks

A dual protection scheme is suggested using both the Hall C BPM system and direct instrumentation of the raster magnet itself. The BCMs would monitor beam position and motion in close to real time and coil voltage monitoring on the raster coils would provide ample early warning of raster problems. Both these independent signals would be fed into the FSD system. Radiator temperature could be monitored to provide a third independent protection system. Thermocouples mounted on the radiator should be robust against radiation damage and should provide fast enough protection against radiator overheating.

6 Safety Documentation and ERR process

The CPS will be required to have an ERR review since it represents a significant new piece of experimental equipment for Hall C with new safety considerations. This review process uses peer review with a combination of Lab and outside experts to study the safety implications and review design and safety documents. This process has a set of documentation requirements. The experiment itself will have its own set of standard required documents. The CPS does not have any new safety considerations even though it is a unique design. Hall C has had secondary in Hall water cooled dumps before of comparable power. High power radiators are also not new. The combination of a high

power radiator, magnet and beam dump inside a shielded "box" imposes reliability and remote handling considerations and these are the primary engineering controls providing personnel protection. Satisfying the standard experiment documentation and ER process should be completely adequate to insure overall safety of the CPS.

7 Commissioning plan for CPS and testing

A full pre-assembly and test of the CPS magnet, shielding cooling system and DC power is suggested. The goals of this pre-assembly and test are to verify fit of all components and to verify via life testing the magnet performance and cooling system. Simulations of various magnet failure modes such as reduced water flow, no water flow, overheating etc. etc. can be used to proof test instrumentation. Interlocks and controls. These tests would be repeated in Hall C after final installation and assembly.

8 Closed cycle CPS Cooling

Activation of the cooling water of the CPS magnet and beam dump is likely and a closed cycle cooling system is suggested. The magnet heat and dump heat can be removed thru a heat exchanger to either the Hall C air or LCW. Any activation of the CPS will be confined to a very small volume and in the event of a leak external contamination will be minimized. A leak pan under the CPS could easily be included to catch and confine any leakage up to and including a total loss of primary coolant. A modular pallet mounted design would be efficient and would include primary coolant pumps, DI resin beds, heat exchanger, surge tank, controls, instrumentation and manifolds.

9 Post Experiment Removal Plan for CPS

The CPS is expected to become activated and contaminated by the completion of the experiment. Exposure to Hall C staff will be minimized by designing the CPS for a one-piece removal using a large truck crane. This eliminates the need for staff to dis-assemble the CPS. Water disconnects using self-sealing connectors can be used to eliminate any primary cooling water loss. The DC Power supply and air-cooled cables will be disconnected and removed as they are not expected to be activated. The CPS will be removed from hall C by truck to a safe storage location. The cooling water pumps, controls, DI resin beds and heat exchanger will likely have contaminated water inside but will not otherwise be activated. The cooling pallet can be removed to storage intact or the water drained and stored separately or disposed of.

10 Cost Analysis

Preliminary cost analysis has be made by using vendor quotations for W-powder and actual cost for the similar size normal conducting magnets.

- Tungsten powder shield, 64 tons, $2400k
- The magnet yoke with permedur poles, 1.5 tons, $10k + $30k
- The coils with kapton tape isolation, $30k
- Cu core absorber and closed loop water cooler, $25k
- The WCu(20%) insert, 1 ton, $100k
- Support structure and the elevation jacks, $50k
- The beam line, radiator, and raster magnet with power supply, $50k
- New Girder and rebuild estimate, 50K$
- closed cycle magnet and dump cooling system, 25 K$
- Instrumentation, controls, interlocks, PLC, 50K$
- Rented crane and crew 5K$/day (depends on crane size)

A total cost was found to be significant $2.7M where the tungsten is a dominating part. Alternative shielding material is surplus lead which could be obtained (Oct. 2017) from SLAC for relatively low cost. However, it will increase the weight of the CPS from 75 tons to 155 tons.

---

[1] D. Hamilton, "Photon Beam Requirements for Wide-Angle Compton Scattering", in arXiv:1704.00816.

[2] D. Keller, "The UVa approved and proposed experiments", in arXiv:1704.00816.

[3] B. Wojtsekhowski and G. Niculescu, "Conceptual Design Report, A Compact Photon Source", Supplementary material for the WACS proposal PR12-15-003 to the JLab PAC 43, June 2015; in arXiv:1704.00816.

[4] P.K. Kloeppel, "Design for 25-kW beam dumps at 100 MeV and 500 MeV", CEBAF-TN-90-205; M. Wiseman, C.K. Sinclair, R. Whitney, M. Zarecky, "High Power Electron Beam Dumps at CEBAF".

Appendix 1: Concept Transfer to Hall D

The intense photon source is one component of the K_L beam. The experimental method can be summarized as follows: electrons hit a copper radiator, the resulting photons hit a Be target, and a beam to K_L is produced. The search for missing hyperons is a strong motivation for this setup.

The new setup utilizes the Hall D Tagger vault, properly shielded by design to accomodate the medium power beam dump capable of accepting up to 60 kW of 12 GeV electron beam, assuming that proper local shielding is set around the dump. The presently

installed dump is placed behind the iron labyrinth walls, and is surrounded by a massive iron shielding, made of iron blocks available at the time of construction. The standard GlueX setup is optimized for operations using very thin radiators producing relatively low intensity photon beam such that the beam electrons losing energy to photon production in the radiator may be detected and counted in the tagger hodoscope counters. The present setup is not suitable for production of massively more intense photon beams needed for the K_L production, due to the expected overwhelming radiation and activation levels in the vault.

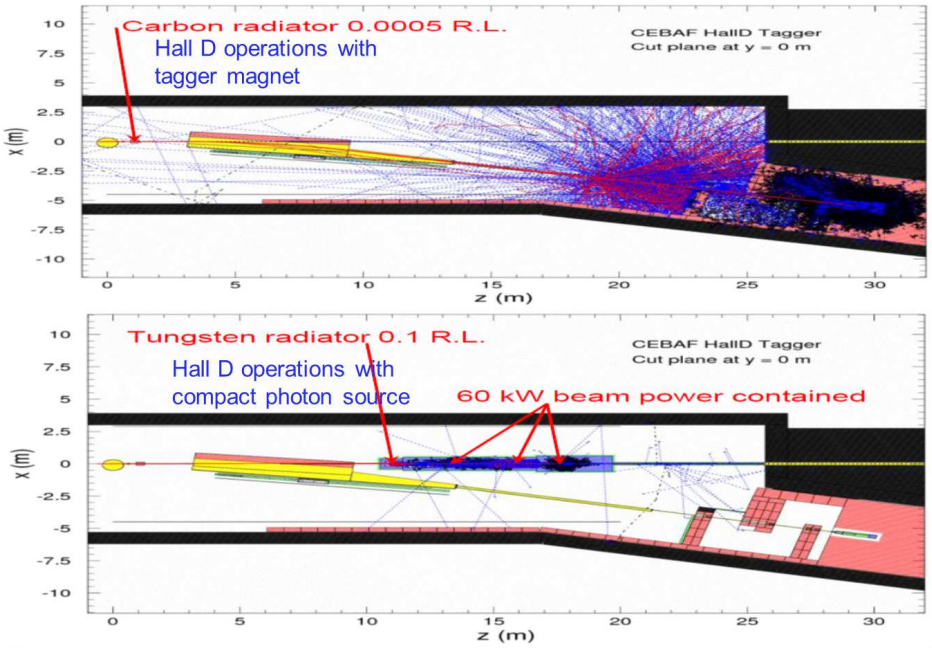

Figure 27. 2D projection of backgrounds in the Hall D alcove for both, the nominal GlueX beam/dump and the 5μA/CPS configuration.

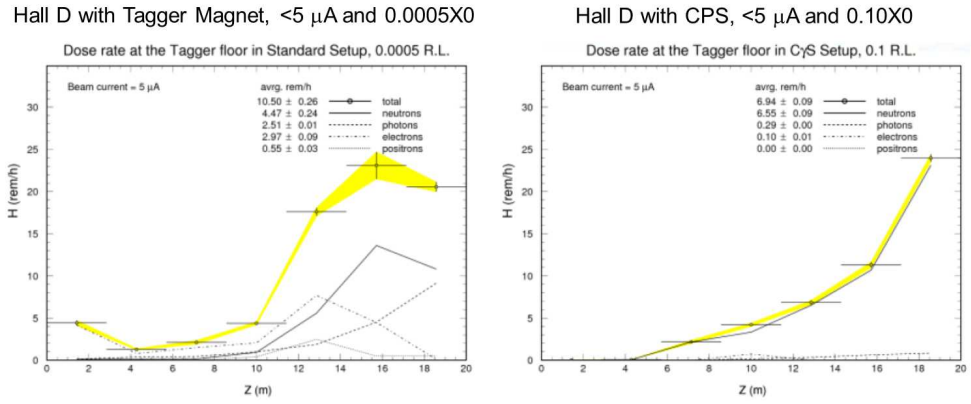

Figure 28. Dose rate at the tagger in standard configuration (left) and with CPS and 10% radiator (right). The CPS with its optimized shielding design does not increase radiation levels beyond standard configuration.

The CPS will be located downstream of the tagger magnet. The tagger alcove has more space than that available in Hall A/C, so positioning and shielding placement are simpler. Indeed, the CPS implementation in Hall D may have a different length and magnet field, as well as shielding. A total floor loading of the implementation up to 100t is acceptable. If one uses a 2nd raster system for Hall D to compensate for the initial 1mm rater, this can be an equivalent essential design to the Hall C/A one.

As discussed in section IV, the Compact Photon Source converts beam energies of up to 12 GeV with currents of up to 5 μA into a high-intensity source of collimated photons. For the Hall-D adaptation, the 5 μA beam current is limited by the design of the Hall D Tagger Magnet alcove. This corresponds to a 60 kW power limit. Note that the ceiling shielding of the Tagger hall above the CPS position is the same as it is above the existing 60 kW dump. No radiation increase at the site boundary is thus expected with respect to 60 kW operations using the existing dump. Figs. 27 and Fig. 28 illustrate how the CPS stops the electron beam and absorbs almost all beam energy inside, and therefore provides excellent shielding. Running the CPS at full beam power produces radiation fields in the Hall D tagger area, comparable with running regular Hall D experiment utilizing a very thin radiator in front of the tagger magnet.

Appendix 2: Benchmark comparison

From the engineering standpoint, two of the most important aspects in the design and subsequent building of a Compact Photon Source are the ability to properly shield the radiation produced inside the source and to dissipate the resulting heat in a safe manner. While the latter point was addressed earlier in this document, in this Appendix we focus on the former issue, specifically detailing the steps taken to benchmark the simulations used in assessing the prompt, as well as the residual (activation) radiation level around the CPS and in the experimental Hall. Even though they have been mentioned before, it is worth reiterating the basic radiation level constraints associated with experiments at JLab:

From the radiological protection point of view the following set of limitations should be satisfied, conservatively assuming typical expected experimental run conditions:

- Beam energy: 11.5 GeV Beam electron beam
- Current: 2.6 μA
- Beam Power (based on the above) = 30 kW
- Run time: $\sim$ 1000 hours

For the typical, high current JLab experiment the radiation dose rate parameters must stay within the following limits:

- Dose rates in the Hall should be under several rem/h at 10 m from the device
- Dose rates at the boundary should be under 1 $\mu rem/h$ during the run

- Dose rates outside the device envelope at a foot distance from the device should be under several $mrem/h$ after one hour following the end of the 1000 hour run

In order to gain an understanding of the radiation levels likely to be produced by the CPS and to ultimately design the optimal shielding for it, one relies on Monte Carlo simulations and over the years the nuclear and particle physics community[1] has developed a series of very sophisticated simulation programs. In time these programs became more complex, with several physical processes that can be turned on and off, various thresholds and cutoffs that might greatly influence the result yet they are buried deep inside the code. Therefore, one has to be careful in using and interpreting the results of such simulations because, as suggested above, the same simulation can give vastly (i.e. orders of magnitude differences) different results with only (seemingly) minor changes in the input parameters.

Ideally one would want to **ground–truth** the simulation by **experimentally measuring** a small but relevant setup and verify that the simulation results agree with the measured radiation levels of that setup. For the current study this step was not done explicitly, though one can argue that one of the simulation programs used (Geant3) was extensively **ground–thruth–ed** as the JLab RadCon group compares the radiation levels measured at boundary of the experimental Halls with the Geant3 predictions.

To benchmark the simulations used in the CPS design a couple of relatively simple radiation scenarios were independently simulated using three different simulation programs (Geant3[2], Fluka[3], and Geant4[4]) by the three groups involved in this process, as follows:

- JLab group (led by P.D.): used Geant3
- UVa group (led by J.Z.): used Fluka
- JMU group (led by G.N.): used both Geant4 and Fluka

The geometry that was simulated was a simple sphere with a small cylindrical hole bored in it such that the 30 kW, 11.5 GeV beam interacts inside the sphere (at $z = 30$ cm for the Fe sphere and at $z = -15$ cm for the W sphere).

	Dose Rates [mrem/h]								
	JLab DINREG/Geant3			JMU Geant4			UVa Fluka		
	n	γ	total	n	γ	total	n	γ	total
3 m Fe	146	0.44	146.44	123.2	0.56	123.76	10	0.039	10.039
3 m Fe + Poly- B	0.8	2.8	3.6	0.284	0.56	0.844	0.11	0.063	0.173
1.5 m W	13	0.06	13.1	6.34	0.33	6.67	1.7	0.0002	1.7002
1.5 m W+Poly-B	2.7	0.003	2.7	1.76	1.28	3.04	0.15	0.0007	0.1507

Table I. Geant3, Fluka, and Geant4 prompt radiation comparison for Fe and W spheres.

[1] As well as related areas such as nuclear medicine, astronomy, defense, etc.

[2] The only code currently setup for calculating the radiation at the JLab boundary is Geant3.

[3] Fluka is the only choice for activation calculations.

[4] The development of the Fortran–based Geant3 code has ceased long time ago and the community has/is migrating toward the C++ based Geant4.

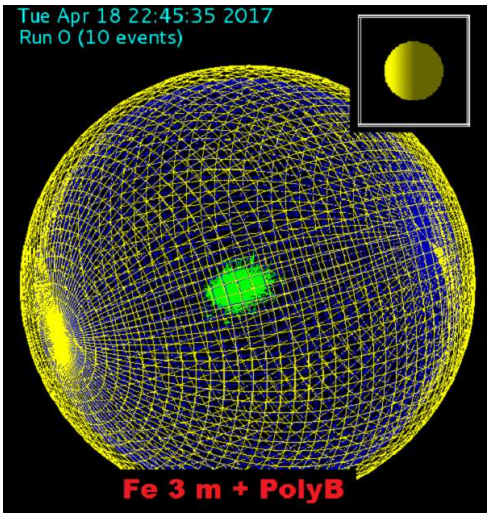

Figure 29. Fe sphere with the Borated Poly layer, as simulated in Geant 4.

Four of these setups were simulated:

- A 300 cm diameter **Fe** sphere
- A 150 cm diameter **W** sphere
- A 300 cm diameter **Fe** sphere with an outer 10 cm Borated Polyethylene layer (5 % Boron by weight
- A 150 cm diameter **W** sphere with an outer 10 cm Borated Poly layer

The results of these parallel simulations are summarized in the Table below.

Examining these results one notes the reasonable agreement between the Geant3 and Geant4 simulation, though factors of 1–2 could not be ruled out in the differences (and are to be expected in these types of estimations). The radiation levels predicted for these spheres leads one to conclude that the optimization of the CPS shielding satisfying the safety requirements in the Halls and outside ought to be possible. The addition of a borated polyethylene layer seems to be absolutely critical in moderating and absorbing low energy neutrons. This becomes very important if one choses[5] Fe as (part of) the shielding material.

One notes that a dose rate of $\sim$2.4 $\mu rem/h$ at the boundary correspond to a "regular" normal experiment, not requiring extra shielding measures, corresponding to about the "200% of allowable design boundary dose rate" (that is, the dose rate at which the dose accumulation would be 10 mrem if such conditions are run for a half of the calendar year continuously).

The Fluka simulation (carried out in parallel at UVa and at JMU) was able to provide residual radiation (due to activation) at various time intervals: 1 hour, 24 hours, 7 days, 30 days. Sample results for the 3 m Fe sphere, one hour after the end of the irradiation cycle (assumed to be 1000 hours of 11.5 GeV, 2.6 μA beam) are shown in the Figures below.

[5] For example for cost containment.

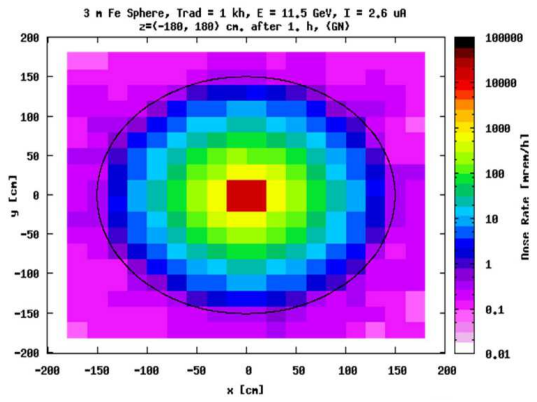

Figure 30. Radiation level one hour after the end of the irradiation period. Closeup view of the JMU Fluka result.

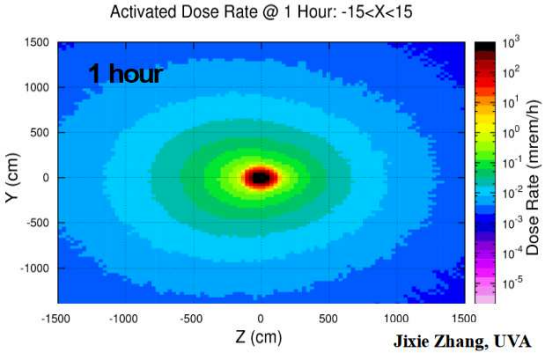

Figure 31. Expanded view of the radiation level one hour after the end of the irradiation period (UVa Fluka result). Both plots correspond to the 3 m Fe sphere.